Journal of Nuclear Medicine, published on July 13, 2017 as doi:10.2967/jnumed.117.193250

Curative multi-cycle radioimmunotherapy monitored by quantitative SPECT/CT-based theranostics, using bispecific antibody pretargeting strategy in colorectal cancer

Sarah M. Cheal[1,2], Edward K. Fung[3], Mitesh Patel[2], Hong Xu[4], Hong-fen Guo[4], Pat B. Zanzonico[3], Sebastien Monette[5], K. Dane Wittrup[6,7,8], Nai-Kong V. Cheung[2,4], Steven M. Larson[1,2]

[1]Department of Radiology, Memorial Sloan Kettering Cancer Center, New York, NY

[2]Molecular Pharmacology Program, Memorial Sloan Kettering Cancer Center, New York, NY

[3]Department of Medical Physics, Memorial Sloan Kettering Cancer Center, New York, NY

[4]Department of Pediatrics, Memorial Sloan Kettering Cancer Center, New York, NY

[5]Tri-Institutional Laboratory of Comparative Pathology, Memorial Sloan Kettering Cancer Center, Weill Cornell Medicine, and The Rockefeller University, New York, NY

[6]Department of Chemical Engineering, Massachusetts Institute of Technology, Cambridge, MA

[7]Department of Biological Engineering, Massachusetts Institute of Technology, Cambridge, MA

[8]Koch Institute for Integrative Cancer Research, Massachusetts Institute of Technology, Cambridge, MA

Corresponding author: Steven M. Larson, MD, Memorial Sloan Kettering Cancer Center, 415 East 68th Street, Z-2064, New York, NY 10065 USA

Phone: 646-888-2212. Fax: 646-717-3263. Email: larsons@mskcc.org

First author: Sarah M. Cheal, PhD, Memorial Sloan Kettering Cancer Center, 417 East 68th Street, New York, NY 10065 USA
Phone: 646-888-2220. Fax: 646-717-3263. Email: cheals@mskcc.org

Running title: Curative theranostic pretargeting of CRC
Word counts: 350 (abstract), 4,983 (full text)
Keywords: Pretargeting, Colorectal Cancer, Radioimmunotherapy, SPECT

ABSTRACT

Radioimmunotherapy of solid tumors using antibody-targeted radionuclides has been limited by low therapeutic indices (TI). We recently reported a novel three-step pretargeted radioimmunotherapy (PRIT) strategy based on a glycoprotein A33 (GPA33)-targeting bispecific antibody (bsAb) and a small-molecule radioactive hapten, a complex of lutetium-177 (^{177}Lu) and *S*-2-(4-aminobenzyl)-1,4,7,10-tetraazacyclododecane tetraacetic acid (^{177}Lu-DOTA-Bn) that leads to high TIs for radiosensitive tissues such as blood (TI = 73) and kidney (TI = 12). We tested our hypothesis that a fractionated anti-GPA33 DOTA-PRIT treatment regimen calibrated to deliver a radiation-absorbed dose to tumor >100 Gy would lead to a high probability of tumor cure while being well tolerated by nude mice bearing subcutaneous GPA33-postitive SW1222 xenografts. **Methods:** We treated groups of nude mice bearing 7-day-old SW1222 xenografts with a fractionated three-cycle anti-GPA33 DOTA-PRIT treatment regimen (total administered ^{177}Lu-DOTA-Bn activity: 167 MBq/mouse; estimated radiation-absorbed dose to tumor: 110 Gy). In randomly selected mice undergoing treatment, serial single-photon emission computed tomography/computed tomography (SPECT/CT) imaging was used to monitor treatment response and calculate radiation-absorbed doses to tumor. Necropsy was done on surviving animals 100-200 days post-treatment to determine frequency of cure and assess select normal tissues for treatment-related histopathologies. **Results:** Rapid

exponential tumor progression was observed in control treatment groups (i.e., no treatment *or* ^{177}Lu-DOTA-Bn only), leading to euthanasia due to excessive tumor burden, while 10/10 complete responses were observed for the DOTA-PRIT treated animals within 30 days. Treatment was well tolerated and 100% histologic cure in 9/9 assessable animals without detectable radiation damage to critical organs, including bone marrow and kidney. Radiation-absorbed doses to tumor derived from SPECT/CT (102 Gy) and from biodistribution (110 Gy) agreed to within 6.9%. Of the total dose of ~100 Gy, the first dose contributes 30%, the second dose 60%, and the third dose 10%. **Conclusion:** In a GPA33-positive human colorectal cancer (CRC) xenograft mouse model, we validated a SPECT/CT-based theranostic PRIT regimen that led to 100% complete responses and 100% cures without any treatment-related toxicities, based on high TIs for radiosensitive tissues. These studies support the view that anti-GPA33 DOTA-PRIT will be a potent radioimmunotherapy regimen for GPA33-positive CRC tumors in man.

INTRODUCTION

Radioimmunotherapy has been investigated for decades as a promising therapeutic strategy for selective targeting of ionizing radioisotopes to liquid and solid tumors in man (*1*). Few successes in safely and effectively treating tumors by this approach have been achieved in solid tumors (*1*). An effective radioimmunotherapy approach would address a major unmet need, especially for patients with advanced metastatic CRC, a cancer with a five-year survival of only 11%. Unfortunately, numerous clinical investigations of radioimmunotherapy against CRC-associated antigens have yielded limited clinical benefit, irrespective of radioisotope used (*1*). The main hurdle observed was insufficient radiation delivery to tumor at radioimmunotherapy activities compatible with body tolerance. Maximal treatment benefits reported thus far using radioimmunotherapy with whole IgG have been stabilized tumor growth in a minority of treated patients, and calculated radiation-absorbed doses have been relatively low; for example, the use of ^{131}I-huA33 to target GPA33 in CRC resulted in modest tumor doses ranging from 12 to 33 Gy at the maximum tolerated dose of 1480 MBq/m^2, without cure in small tumors, and with a corresponding mean red marrow-absorbed dose of ~122 cGy (TI ~16) (*2, 3*).

TI in radioimmunotherapy can be greatly improved by using a multistep method, such as the pre-targeting approach, based on the discovery of Reardan, et al., that antibodies could be developed against metal chelates (*4*). This allowed for

the separation of the antibody-based tumor targeting step from the radioactive small molecular hapten component. Additional improvements in targeting to tumor were achieved by modifications, such as the use of streptavidin by Axworthy and colleagues (*5*). However, these ultimately failed based on serious practical drawbacks related to immunogenicity of reagents and low TI (see (*1*) for a review).

In response to these limitations, Orcutt et al. used mathematical modeling to estimate that a hapten-binding antibody must have affinity of <100 pM for efficient delivery of ionizing radiation in PRIT (*6*), and developed a novel PRIT approach called "DOTA-PRIT" (Fig. 1). The primary features include: (a) the modular bsAb format (IgG-scFv) offers multivalent and simultaneous antibody binding of two distinct antigens: a tumor antigen and the pM affinity anti-DOTA hapten antibody fragment C825 that recognizes small radioactive yttrium- or lutetium-chelate complexes of DOTA-Bn (*6*); and (b) the use of radio-haptens (e.g., ^{177}Lu-DOTA-Bn) with almost exclusive renal clearance and with negligible retention in normal tissue (*7*)).

The purpose of this study was to investigate the efficacy and toxicity of a three-cycle fractionated DOTA-PRIT treatment capable of delivering an absorbed dose of >100 Gy to subcutaneous human CRC tumor xenografts. We report our results with ^{177}Lu, a theranostic isotope that enables non-invasive treatment monitoring and dosimetry in combination with therapeutic β-emission ($t_{1/2}$ = 6.7

days; E_{max} = 0.5 MeV; $E_{average}$= 0.13 MeV; max range = 1.5 mm). The γ-emissions of ^{177}Lu (208 and 113 keV, with 10% and 6% abundance, respectively) enable direct quantitative theranostic SPECT imaging during treatment. A sub-aim was to validate the SPECT imaging component of DOTA-PRIT for direct tumor dosimetry, on a treatment cycle-specific basis.

MATERIALS AND METHODS

Reagents and General Procedures

The anti-GPA33 DOTA-PRIT bsAb huA33-C825 (210 kDa) was expressed and purified as described by Cheal et al (*8*). A treatment cycle of anti-GPA33 DOTA-PRIT consisted of three separate intravenous injections via the tail vein: 0.25 mg of huA33-C825 at t = -28 h, then 62.5 μg of clearing agent at t = -4 h, and 55 MBq of ^{177}Lu-DOTA-Bn at t = 0 (*8*). The GPA33(+) human CRC cell line SW1222 was obtained from the Ludwig Institute for Cancer Immunotherapy (New York, NY) and grown by serial passage. All animal experiments were done in accordance with protocols approved by the Institutional Animal Care and Use Committee of MSK, following National Institutes of Health guidelines for animal welfare. Please see Supplemental Data for additional technical details regarding cell culture and animal models.

DOTA-PRIT Treatment Regimen

Mice bearing subcutaneous SW1222 xenografts (30-170 mm^3, 7 d after inoculation) with either: no treatment (n = 5; tumor volume = 114 ± 35 mm^3), ^{177}Lu-DOTA-Bn only (n = 5; tumor volume = 128 ± 34 mm^3; two cycles, total administered ^{177}Lu-DOTA-Bn activity: 110 MBq), or a three-cycle DOTA-PRIT regimen consisting of anti-GPA33 PRIT + 55.5 MBq of ^{177}Lu-DOTA-Bn (n = 10; tumor volume = 83 ± 38 mm^3; total administered ^{177}Lu-DOTA-Bn activity/mouse: 167 MBq). For DOTA-PRIT, cycle 1 was given on days 7 and 8 post-tumor inoculation. This was repeated 6 days later (i.e., weekly) with cycle 2 given on days 14 and 15, and cycle 3 given on days 21 and 22. All groups were monitored 2-3 times per week for overall health, body weight, and measurement of tumor burden by external caliper, with tumor volume calculated using the volume of an ellipsoid. Mice were sacrificed when the tumor volume exceeded 2500 mm^3 (or earlier if the tumor burden interfered with mobility), or if excessive weight loss (>25%) from pre-treatment baseline was noted. Tumor growth was analyzed by performing a non-linear regression fit of an exponential growth curve to the tumor volume data collected in the first 21 days following tumor inoculation for the non-treated and treatment with ^{177}Lu-DOTA-Bn only groups. The tumor growth data of the animals treated with the three-cycle DOTA-PRIT regimen were fitted by an initial exponential growth curve up to and including day 14 (i.e., onset time of growth delay and shrinkage) using GraphPad Prism version 6.00.

Monitoring of DOTA-PRIT Treatment with SPECT/CT

Five randomly selected mice undergoing anti-GPA33 DOTA-PRIT treatment underwent serial non-invasive SPECT/CT imaging for verification of tumor targeting and calculation of tumor dosimetry. Each animal was imaged 5-6 times at various time points during fractionated treatment, up to 24 h post-injection (p.i.) of cycle 3 with ^{177}Lu-DOTA-Bn (day 23) (Fig. 2). For each image, tumor volumes were estimated by CT image analysis, and the total activity in the tumor region was estimated by SPECT image analysis. Tumor count rates were converted to activity concentrations (MBq per gram (g)) using a measured system calibration factor for ^{177}Lu. Additional technical details regarding SPECT/CT imaging, corrections and dosimetry calculations can be found in the Supplemental Data.

Necropsy of Animals That Underwent DOTA-PRIT Treatment

Mice were euthanized with CO_2 according to the guidelines of the American Veterinary Medical Association. Following gross examination, organs were fixed in 10% neutral buffered formalin. After fixation, bones were decalcified in a formic acid solution (Surgipath Decalcifier I, Leica Biosystems). Fixed organs were further processed for histology in ethanol and xylene in a Leica ASP6025 tissue processor and embedded in paraffin. Paraffin blocks were

sectioned at 5 microns, stained with hematoxylin and eosin, and examined by a board-certified veterinary pathologist (SM). The following tissues were examined: skin and subcutaneous tissue from tumor implantation site, liver, kidney, spleen, and bone marrow (sternum, vertebrae, femur, and tibia). Hematology and serum chemistry was also collected for each mouse; please see Supplemental Data for technical details. Any abnormal gross or histologic findings were noted.

Statistical Analysis

Kaplan-Meier survival analysis or statistical comparisons between groups (Student's *t* test) were performed with Prism software (version 6.0; GraphPad Software). For all studies, the level of statistical significance is set at $P < 0.05$.

RESULTS

Fractionated Treatment with DOTA-PRIT

No significant difference in average tumor volumes was found among the three groups at the start of treatment. Tumor sizes measured over the course of the experiment demonstrate a clear difference in efficacy between the control treatment groups (i.e., no treatment *or* ^{177}Lu-DOTA-Bn only) and the DOTA-

PRIT treated groups. This is shown in Fig. 3a where tumor volumes are plotted as a function of time after xenograft inoculation for all treatment groups.

Kaplan-Meier plots, shown in Fig. 3b, were generated for all three groups. Development of a 1000 mm^3 tumor volume that necessitated euthanasia due to excessive tumor burden was designated as the "survival" endpoint. All untreated mice and mice treated with ^{177}Lu-DOTA-Bn only (10/10, 100%) developed very large, exponentially growing tumors, requiring euthanasia of the animals. Individual tumor doubling times ranged from 3.6 to 6.0 days (R^2 = 0.90-0.99). Because of this rapid tumor growth, treatment with ^{177}Lu-DOTA-Bn only was limited to just two cycles. The median time to a terminal 1000 mm^3 tumor volume was 19 days for no treatment, and 16 days for treatment with two cycles of ^{177}Lu-DOTA-Bn only. For all DOTA-PRIT treated mice (10/10, 100%), the tumors grew exponentially to a maximum size of 247-386 mm^3 on day 14 (tumor doubling time range: 2.2-5.1 days; R^2 = 0.82-0.99). Following the third cycle of treatment (administered on days 21-22, post-tumor inoculation), tumors showed rapid regression to below the palpable threshold ($\leq$ 10 mm^3) by approximately day 30 (Fig. 3a). Tumor volumes at the start of cycles 2 and 3 were 298 $\pm$ 51 mm^3 and 31 $\pm$ 19 mm^3, respectively, measured manually by caliper. For the DOTA-PRIT treated mice, median time to the terminal 1000 mm^3 tumor burden was never reached since all animals showed complete responses with no recurrence before study endpoints (118-200 days post-inoculation) in 10/10 animals. By log-

rank (Mantel-Cox) test, survival of the DOTA-PRIT group was significant ($P < 0.0001$).

SPECT/CT Imaging to Monitor Treatment and Quantify Tumoricidal Tumor Doses

SPECT/CT of tumor-bearing mice undergoing treatment demonstrated highly selective tumor localization of pretargeted ^{177}Lu-DOTA-Bn as early as 1 h p.i. of ^{177}Lu-DOTA-Bn. At this time, the average effective ^{177}Lu activity concentration in tumor (as average megabecquerel per gram of tumor (MBq/g) ± SD; $n = 4$) was 3.92 ± 0.85 MBq/g, corresponding to an uptake of injected ^{177}Lu-DOTA-Bn of 7.1 ± 1.5 % per g of tumor volume. Prolonged and high tumor retention of ^{177}Lu activity was also observed when imaged at 24 and 160 h p.i. (non-decay-corrected activities: 3.17 ± 1.10 and 0.64 ± 0.19 MBq/g), suggesting minimal biological clearance of ^{177}Lu activity from the tumor. Activity in the bladder region is apparent in the SPECT images at 1 h p.i., consistent with renal clearance of free ^{177}Lu-DOTA-Bn (data not shown). Rapid renal clearance of free ^{177}Lu-DOTA-Bn was also supported by the observation that whole-body activity of each individual animal, determined by assay in a dose calibrator, was similar to the measured tumor-associated activity. ^{177}Lu activity remaining in the mice measured after 24 h and 160 h p.i. of cycle 1 (as average ± SD; $n = 5$) was 6.98 ± 1.64% and 1.18 ± 0.39% of administered activity, respectively. Although the

SPECT/CT imaging demonstrates that the most prominent focus of activity was in the tumor, very low levels of ^{177}Lu activity were detected in the liver, spleen, and kidney (~10- to 15-fold less activity than tumor, as percent injected dose per gram of tissue, based on previous biodistribution studies). For cycle 2, the whole-body percentage of administered ^{177}Lu activity remaining after 24 h and 160 h p.i. was 12.83 ± 2.01% and 1.98 ± 0.44%, respectively. Finally, for cycle 3, the whole-body percentage of administered ^{177}Lu activity remaining after 24 h was 4.81 ± 1.03% (note: no additional data was collected for cycle 3 after 24 h).

The CT image-derived tumor volumes (in mm^3) demonstrating tumor doubling followed by regression are shown in Table 1. SPECT image-derived ^{177}Lu activity estimates for tumor regions of interest are shown in Table 2 and Figure 4. Tumor dosimetry was calculated from ^{177}Lu time-activity curves and is presented in Table 3. Representative serial SPECT/CT images originating from the same animal are provided in Figure 5. The contribution to total dose was estimated to be greatest during cycle 2 (average dose during cycle 2 period = 43.8 Gy, n = 5). The fitted exponential decay curves of the three-cycle treatment regimen is shown in Fig. 6, illustrating the difference between the measured activity and expected activity from single and two-cycle protocols. Total dose from the three-cycle treatment was estimated at 102 Gy. Radiation-absorbed doses to tumor derived from SPECT/CT (102 Gy) and biodistribution (109.6 Gy) agreed to within 6.9%. For comparison, $[^{177}\text{Lu activity}]_{\text{tumor}}$ for a three-cycle

treatment was simulated based on kinetics derived only from the first cycle of the experimental data. The time-activity curves are shown in Supplementary Figure 1, with tumor dose estimates calculated from the curves shown in Supplementary Table 1. Total tumor dose predicted by the simulation was about 92 Gy, assuming first-cycle kinetics throughout, i.e., the kinetics of subsequent cycles essentially ignore the effects of previous cycles. Measured dose from the three-cycle treatment was higher than predicted.

Toxicity of Fractionated DOTA-PRIT Treatment

All treatments were well-tolerated, with no average weight loss greater than 10% from baseline observation (Supplementary Fig. 2), suggesting no acute toxicity. For DOTA-PRIT treated mice, a slight drop in average weight (~5%) from baseline was observed for the duration of treatment administration, but was reversible to pre-treatment weight about 10 days after the final ^{177}Lu-DOTA-Bn injection. Weight loss was most likely the result of a transient and reversible gastrointestinal toxicity, which did not leave permanent histologic changes, but formal toxicity studies are warranted to verify this. No early, treatment-related deaths were observed.

Histopathology confirmed complete tumor disappearance in all surviving DOTA-PRIT treated mice (9/9) at 3-6 months (96-178 days) post-treatment. No evidence of tumors was observed macroscopically or histologically at the site of

tumor inoculation or in distant organs in 9 of 9 mice that underwent necropsy, consistent with histologic complete cures in those animals (100%).

We found no evidence of treatment-related radiotoxicity in radiosensitive organs in treated animals after either 3 or 6 months post-treatment. For example, in the five mice submitted for necropsy and histopathology assessment at three months post-treatment, no abnormalities, such as bone marrow depletion as seen in ^{177}Lu-IgG radioimmunotherapy (*9*), nephrotoxicity, or increased incidence of mesangial glomerulopathy as seen with ^{177}Lu-peptide-receptor radiotherapy (*10*) treatment, were observed.

A variety of histopathologic changes were noted; these are presented in the Supplemental Table 3. While the majority of these findings were compatible with naturally occurring background lesions typical in mice of this strain and age, two lesions observed with a low incidence were not typical spontaneous lesions. These two lesions, for which a link to test article-induced toxicity could not be ruled out, were: mild to moderate granulomatous hepatitis and/or splenitis (2/9 mice) and marked pulmonary interstitial fibrosis (1/9). Sudden deterioration or death was observed in 2/10 treated animals 136 and 158 days post-treatment. In one animal, this was determined to be due to pulmonary fibrosis of undetermined cause (as mentioned previously) with secondary myocardial hypertrophy; the other mouse could not be analyzed due to the condition of the animal when it was discovered.

DISCUSSION

We herein report a three-cycle, curative theranostic regimen with minimal toxicity for SW1222, a human solid CRC xenograft, derived from a patient with a moderately well differentiated adenocarcinoma of the colon (classification: Dukes' stage C, a locally invasive cancer). There have been extensive pre-clinical studies with multi-step regimens, but the outcome we report, of a high probability (100%) of histologic cures without detectable radiosensitive organ toxicity, is to the best of our knowledge, extremely unusual. Our preclinical development focus has been on hitting therapeutic benchmarks, which must be achieved in human translational trials as well. These are cumulative dose to solid tumor of >100 Gy; TIs for radiosensitive tissues of >12 (kidney); 70 (bone marrow); and 40 (colon), for example. We chose these benchmarks based on clinical human normal-tissue radiation dose tolerance estimates (*11*), as well as experience gleaned from radiopeptide treatments and related toxicities in man (*1*).

In our preliminary studies with anti-GPA33 DOTA-PRIT and SW1222, dose escalation resulted in progressive tumor response, and that toxicity was not limiting (*8*). At lower tumor doses, (~40-70 Gy), treatment led to complete responses (e.g., we observed 4/4 complete responses for two-cycle treatment regimen of 55.5 MBq per cycle), but was ultimately sub-curative and resulted in two distinct recurrence phenotypes: (1) outgrowth of antigen-positive tumor with

the same rate of growth as controls (seen in 3/4); and (2) a histologic "senescence" pattern that resulted in dormant tumor, in which antigen-expressing cell growth arrested after one to two doublings (seen in 1/4; observed at 140 days post-injection). It is critical to assess long-term outcome after radioimmunotherapy, because we and others (e.g., (*12*)) have shown that late recurrence can occur in this model, with relatively high frequency when treatment is sub-optimal. In this study we found that repeated dose cycles to higher tumor doses were required to achieve 100% histologic cures in 9/9 treated animals available for assessment by necropsy. With the three-dose regimen, we achieved our targets and in this CRC model, we obtained cures with minimal toxicity [mean TIs for tumor-to-normal tissue were ~73 (blood), ~10 (liver), ~10 (spleen), ~12 (kidney), and ~110 (marrow-bearing bone (femur)) when 10,000 cGy was delivered to tumor (see Tables 1-3 for dose estimates)].

DOTA-PRIT should provide an ideal theranostic platform that permits the use of a single radiopharmaceutical entity for both quantitative imaging and therapy, by simply changing the amount of radioactivity administered. The use of non-invasive SPECT has the advantage of providing a tumor radiation estimate for all three doses in the regimen, which is otherwise impossible to achieve by biodistribution (i.e., terminal) studies alone. The absorbed doses to tumor, 10,160 +/ 141 cGy, were estimated using SPECT. We defined and derived the dose contribution from each cycle by calculating the total predicted dose after that

cycle and subtracting what would have been the total dose, had treatment stopped after the previous cycle. Taking these contributions as proportions of the total dose after three cycles cumulated until total regression of the tumor at 496 hours, it turns out that 60% of the dose is from the second cycle, and cycles 1 (30%) and 3 (10%) contribute smaller fractions. This result is non-intuitive but is based on dynamic measured changes in tumor volume expansion, which in turn is based on CT during cycle 1 treatment, followed by rapid regression during cycle 2 in particular (Table 1).

As a novel feature of this work, we determined that the addition of cycle 3 contributed 10% of the total absorbed dose by tumor, which was essential for histologic cure of the 9/9 tumors examined post-treatment. This may relate to the state of the treated tumor at the time the third cycle is added. Such information is crucial for later treatment planning in the clinic and underscores the importance of a multiple-cycle treatment regimen that is closely monitored with theranostics.

CONCLUSION

This study validated a theranostic curative radionuclide therapy regimen with no clear evidence of radiation-induced toxicity in a murine model bearing human CRC solid-tumor xenografts. We demonstrated that three cycles were required to achieve tumor doses >100 Gy and with TIs of >70 for blood and >10 for kidney, we observed no radiation-related toxicity despite high total

administered ^{177}Lu-activity (167 MBq/mouse). Cycle-specific tumor dosimetry was demonstrated using serial SPECT/CT of animals undergoing treatment. Collectively, these preclinical studies support clinical translation of anti-GPA33 DOTA-PRIT.

FINANCIAL DISCLOSURE

S.M.L., N-K.C., and D.W. own stock in Voreyda Theranostics, Inc. Additionally, S.M.C., H.X., S.M.L., and N-K.C. are inventors on an international patent application for "MULTI-SPECIFIC ANTIBODIES WITH AFFINITY FOR HUMAN A33 ANTIGEN AND DOTA METAL COMPLEX AND USES THEREOF," filed on February 9, 2016.

ACKNOWLEDGMENTS

We gratefully acknowledge Mrs. Blesida Punzalan for her technical assistance. This study was supported in part by the Donna & Benjamin M. Rosen Chair (to S.M. Larson), Enid A. Haupt Chair (to N.K. Cheung), The Center for Targeted Radioimmunotherapy and Theranostics, Ludwig Center for Cancer Immunotherapy of Memorial Sloan Kettering Cancer Center (to S.M. Larson) and R01-CA101830 (K.D. Wittrup). S.M. Larson was also supported in part by P50-CA86438. We also acknowledge the NIH/NCI Cancer Center Support Grant (P30 CA008748) for use of the Tri-Institutional Laboratory of Comparative Pathology, Memorial Sloan Kettering Cancer Center, Weill Cornell Medicine, and The Rockefeller University, New York, NY. Technical services provided by the Memorial Sloan Kettering Small-Animal Imaging Core Facility were also supported by Cancer Center Support Grant P30 CA08748 (to C. Thompson). A

Shared Resources Grant from the Memorial Sloan Kettering Cancer Center Metastasis Research Center (to P. B. Zanzonico), which provided funding for the purchase of the NanoSPECT/CT Plus, is gratefully acknowledged. We are also grateful to Ms. Leah Bassity for her editorial assistance.

REFERENCES

1. Larson SM, Carrasquillo JA, Cheung NK, Press OW. Radioimmunotherapy of human tumours. *Nat Rev Cancer*. 2015;15:347–360.
2. Scott AM, Lee FT, Jones R, et al. A phase I trial of humanized monoclonal antibody A33 in patients with colorectal carcinoma: biodistribution, pharmacokinetics, and quantitative tumor uptake. *Clin Cancer Res.* 2005;11:4810–4817.
3. Chong G, Lee FT, Hopkins W, et al. Phase I trial of ^{131}I-huA33 in patients with advanced colorectal carcinoma. *Clin Cancer Res.* 2005;11:4818–4826.
4. Reardan DT, Meares CF, Goodwin DA, et al. Antibodies against metal chelates. *Nature*. 1985;18-24;316(6025):265–268.
5. Axworthy DB, Reno JM, Hylarides MD, et al. Cure of human carcinoma xenografts by a single dose of pretargeted yttrium-90 with negligible toxicity. *Proc Natl Acad Sci USA.* 2000;97:1802–1807.
6. Orcutt KD, Slusarczyk AL, Cieslewicz M, et al. Engineering an antibody with picomolar affinity to DOTA chelates of multiple radionuclides for pretargeted radioimmunotherapy and imaging. *Nucl Med Biol.* 2011;38:223–233.

7. Orcutt KD, Nasr KA, Whitehead DG, Frangioni JV, Wittrup KD. Biodistribution and clearance of small molecule hapten chelates for pretargeted radioimmunotherapy. *Mol Imaging Biol.* 2011;13:215–221.

8. Cheal SM, Xu H, Guo HF, et al. Theranostic pretargeted radioimmunotherapy of colorectal cancer xenografts in mice using picomolar affinity (8)(6)Y- or (1)(7)(7)Lu-DOTA-Bn binding scFv C825/GPA33 IgG bispecific immunoconjugates. *Eur J Nucl Med Mol Imaging.* 2016;43:925–937.

9. Schlom J, Siler K, Milenic DE, et al. Monoclonal antibody-based therapy of a human tumor xenograft with a ^{177}lutetium-labeled immunoconjugate. *Cancer Res.* 1991;51:2889–2896.

10. Wild D, Frischknecht M, Zhang H, et al. Alpha- versus beta-particle radiopeptide therapy in a human prostate cancer model (213Bi-DOTA-PESIN and 213Bi-AMBA versus 177Lu-DOTA-PESIN). *Cancer Res.* 2011;71:1009–1018.

11. Marks LB, Yorke ED, Jackson A, et al. Use of normal tissue complication probability models in the clinic. *Int J Radiat Oncol Biol Phys.* 2010;76(3 Suppl):S10–19.

12. Barendswaard EC, Humm JL, O'Donoghue JA, et al. Relative therapeutic efficacy of (125)I- and (131)I-labeled monoclonal antibody A33 in a human colon cancer xenograft. *J Nucl Med.* 2001;42(8):1251–1256.

FIGURES

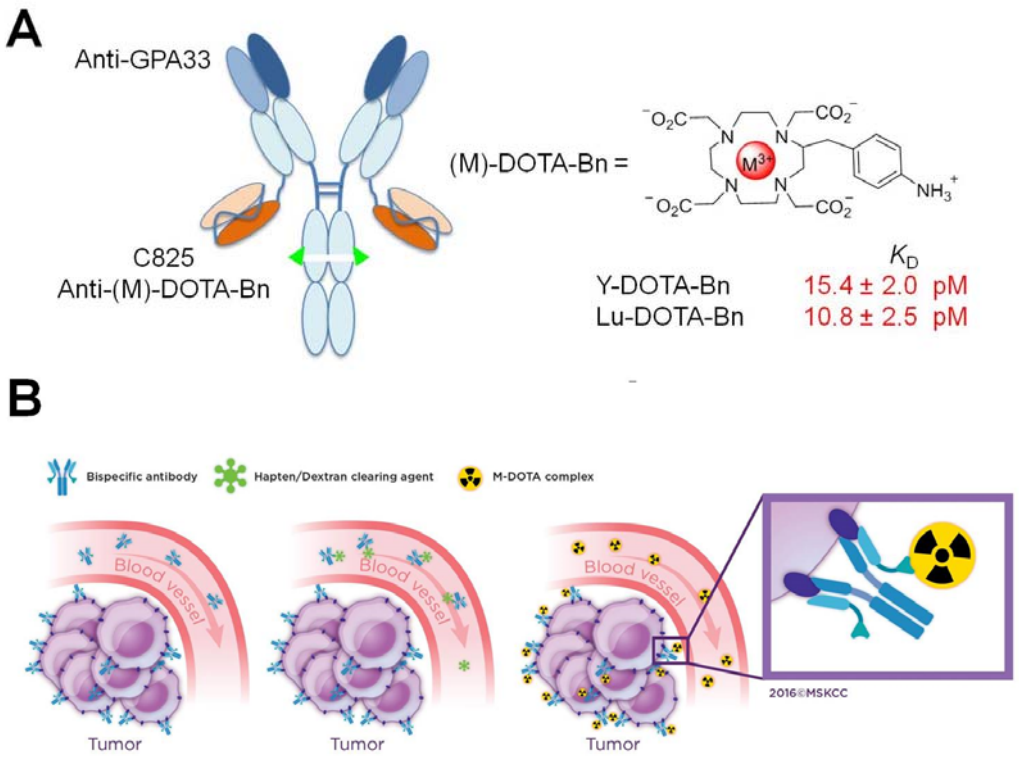

FIGURE 1. Anti-GPA33 DOTA-PRIT concept. (A) Schematic representation of the anti-GPA33 BsAb huA33-C825 (left) and M-DOTA-Bn hapten (right), the vehicle by which ^{177}Lu treatment is administered. The anti-(M)-DOTA-Bn scFv antibody C825 has approximately equal low-pM affinity for either the Y-DOTA-Bn or Lu-DOTA-Bn. (B) Schematic representation of the three-step anti-GPA33 DOTA-PRIT protocol. Copyright 2016, reprinted with permission from Memorial Sloan Kettering Cancer Center (MSK).

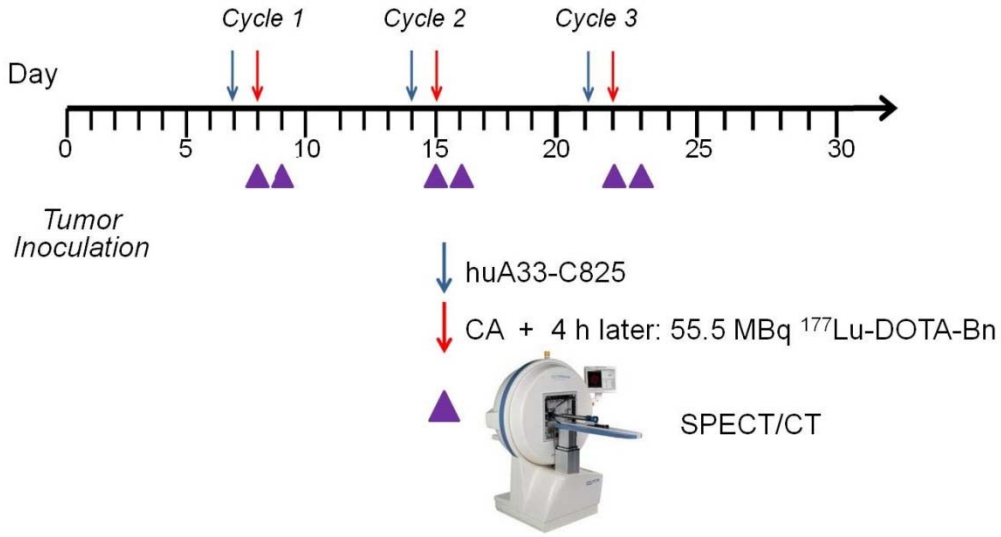

FIGURE 2. Timeline of theranostic anti-GPA33 DOTA-PRIT treatment.

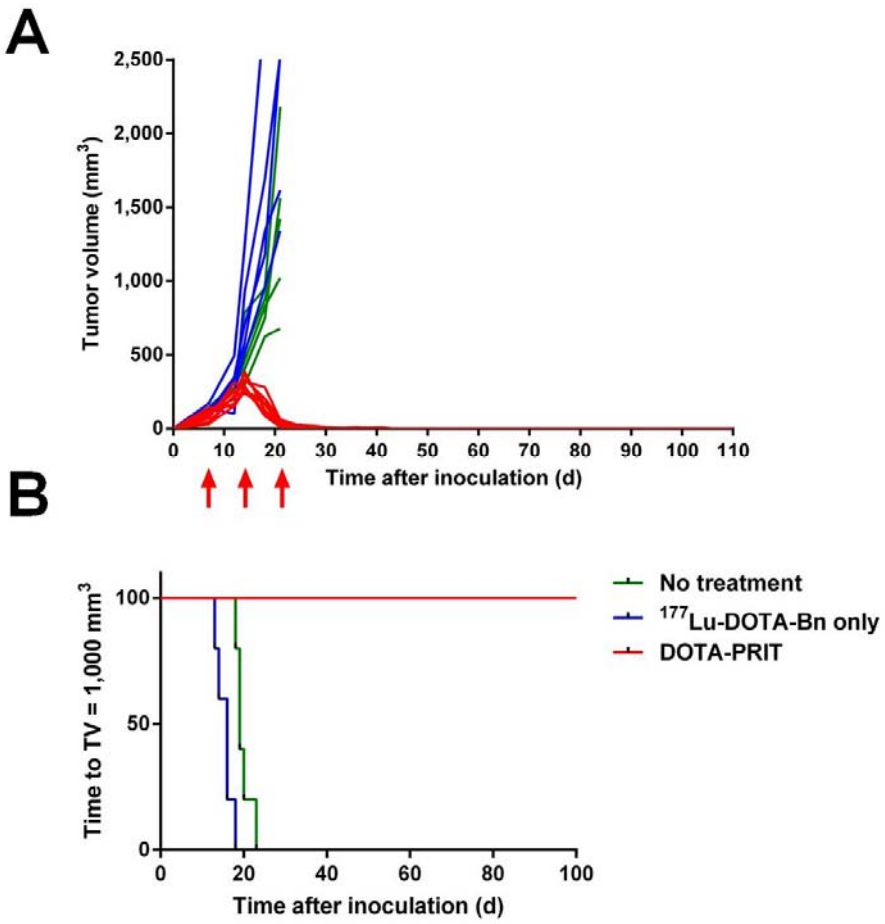

FIGURE 3. Efficacy of DOTA-PRIT evaluated as tumor growth and survival in mice bearing SW1222 subcutaneous xenografts. (A) Tumor growth presented as the change in tumor volume for each individual mouse over time (green: no treatment; blue: ^{177}Lu-DOTA-Bn only; red: DOTA-PRIT). (B) Kaplan-Meier plot of DOTA-PRIT treatment (shown as time to tumor burden of 1,000 mm^3).

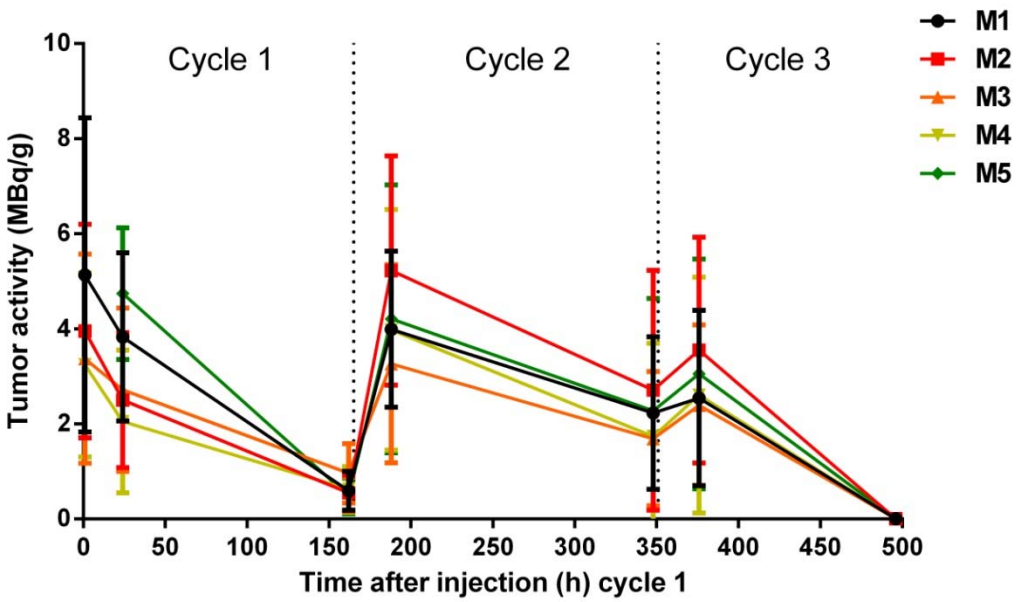

FIGURE 4. Effective (non-decay-corrected) ^{177}Lu activity concentrations (as MBq/g) determined using non-invasive theranostic SPECT/CT imaging during treatment.

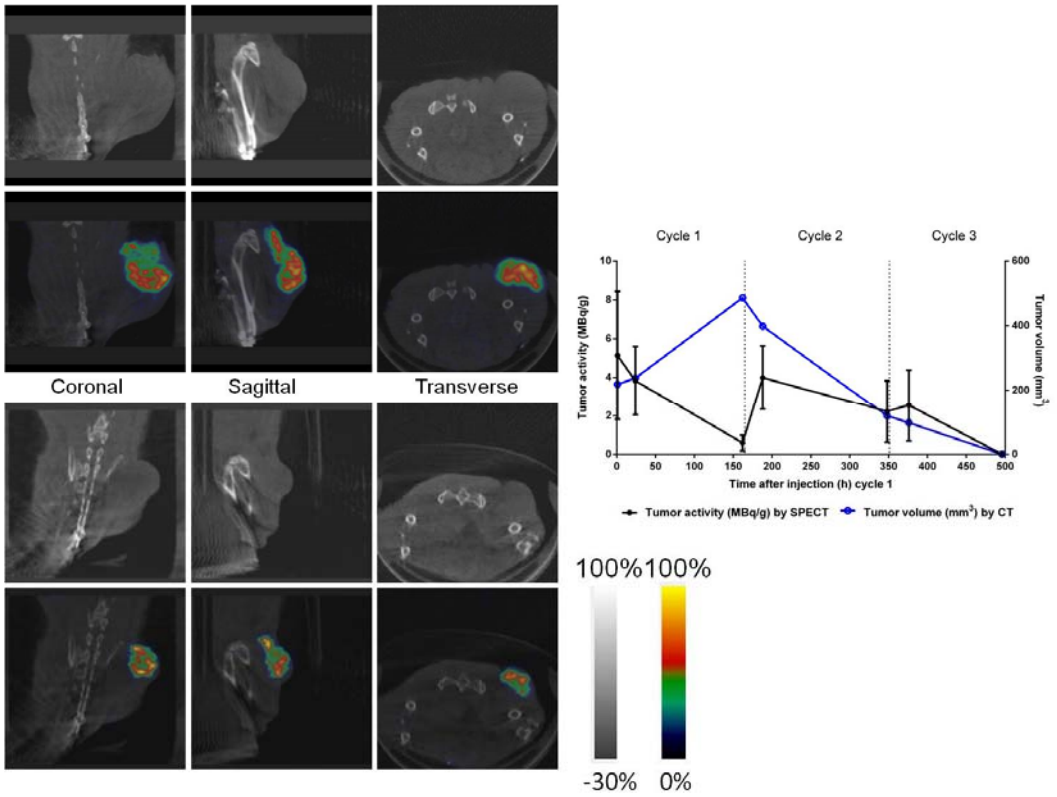

FIGURE 5. Representative SPECT/CT images obtained from same mouse (M1) at 24 hours post-injection of cycle 1 (*top*) and 24 hours post-injection of cycle 3 (*bottom*). A graph depicting the effective tumor activity (as MBq/g) derived from SPECT image analysis (right axis) and tumor volume (as mm^3) derived from CT image analysis (left axis) for this particular animal is provided for reference. For both sets of images, the top rows are CT images and the bottom rows are SPECT/CT fusion images, presented in grey-scale and color-scale, respectively.

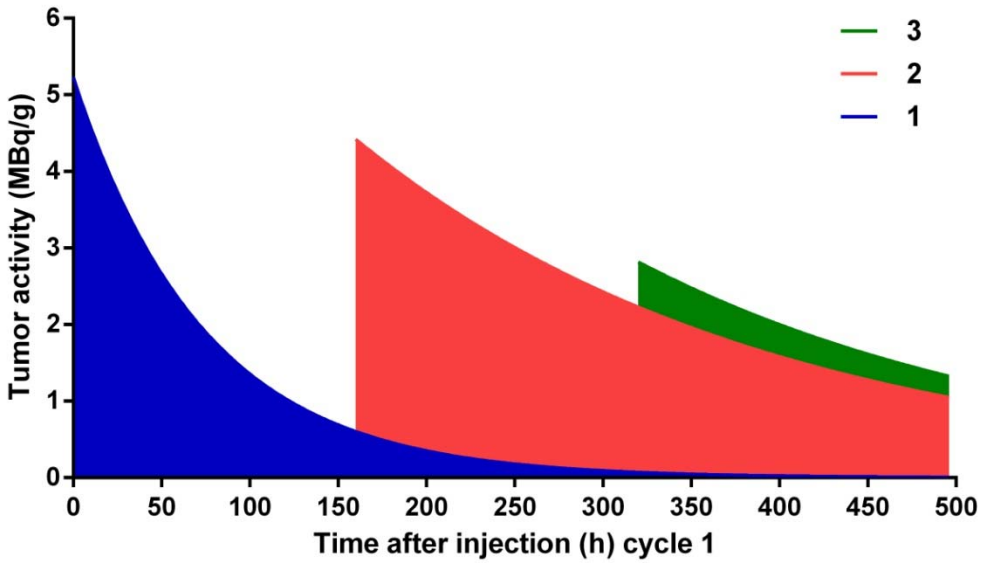

FIGURE 6. Representation of fitted exponential decay curves on three-cycle treatment regimen. Curves were calculated out to complete removal of radioactive label and truncated at 496 hours post-injection of cycle 1, when tumors were no longer grossly palpable. Cumulated dose for cycle 1 represents dose of the blue region, cumulated dose for cycle 2 includes both the blue and red regions, etc. Of the total dose of ~100 Gy, the first dose contributes 30%; the second dose 60%; and the third dose 10% (Table 2).

TABLE 1. CT image-derived tumor volumes (mm^3)

Mouse	Cycle 1, 1 h pi	Cycle 1, 24 h pi	Cycle 1, 160 h pi	Cycle 2, 24 h pi	Cycle 2, 160 h pi	Cycle 3, 24 h pi
1	219	238	486	398	120	97.9
2	168	267	373	318	166	137
3	140	212	206	192	94.3	76.8
4	147	212	193	186	113	99.6
5	N/A	297	291	293	128	94
Average	169	245	310	278	124	101
SD	35.7	36.8	122	89.6	26.5	22.0

TABLE 2. SPECT image-derived ^{177}Lu activity concentrations (not decay-corrected, as MBq/g). N/A = data not collected

Mouse	Cycle 1, 1 h pi	SD	Cycle 1, 24 h pi	SD	Cycle 1, 160 h pi	SD	Cycle 2, 24 h pi	SD	Cycle 2, 160 h pi	SD	Cycle 3, 24 h pi	SD
1	5.14	3.30	3.81	1.77	0.59	0.41	4.00	1.64	2.23	1.60	2.54	1.84
2	3.96	2.25	2.50	1.42	0.55	0.38	5.22	2.41	2.71	2.52	3.55	2.38
3	3.37	2.20	2.72	1.72	0.96	0.63	3.26	2.08	1.69	1.41	2.39	1.69
4	3.24	1.94	2.05	1.50	0.62	0.42	4.00	2.53	1.73	1.96	2.60	2.48
5	N/A	N/A	4.74	1.38	0.48	0.37	4.22	2.82	2.28	2.36	3.05	2.42

TABLE 3. Mean radiation-absorbed doses to xenografts from three-cycle pretargeted ^{177}Lu-DOTA-Bn based on serial SPECT imaging

	Cycle 1		Cycle 2		Cycle 3	
Mouse	Dose 0-160 h (Gy)	Cumulative dose (Gy)	Dose 160-320 h (Gy)	Cumulative dose (Gy)	Dose 320-480 h (Gy)	Cumulative dose (Gy)
1	29.1	32.8	43.5	96.0	27.7	102
2	21.7	24.7	55.5	104	37.7	117
3	25.9	35.4	34.6	77.4	25.4	87.5
4	19.9	24.4	39.9	75.7	26.1	87.4
5	33.4	35.8	45.3	102	32.8	114
Mean	26.0	**30.6**	43.8	**91.0**	29.9	**102**
SD	5.5	**5.7**	7.7	**13.5**	5.2	**14.1**
CoV	21%	18%	18%	15%	17%	14%

Tumors were estimated to be below palpation threshold at 496 h post-injection of cycle 1, thus having an effective activity concentration of zero. Cumulated dose for each cycle was calculated as total dose after 496 h post-injection of cycle 1, assuming treatment was stopped at that dose. Therefore, cycle 2 cumulated dose represents expected dose after 496 hours from a treatment comprising only two cycles. Dose during the third period was calculated from 320 to 480 hours in order to be comparable in duration to the other two periods. In fact, the period after injection of cycle 3 until complete regression of tumor is slightly longer than the other two cycle periods.